International Journal of Minerals*, *Metallurgy and Materials
Volume 18*, *Number 1*, *February 2011*, *Page 105
DOI: 10.1007/s12613-011-0408-y

Processing of refractory materials using various magnesium sources derived from Zinelbulak talc-magnesite

Mirabbos Hojamberdiev[1,2], *Pulat Arifov*[3], *Kamil Tadjiev*[3], *and Yun-hua Xu*[2]

1) New York State College of Ceramics, Alfred University, Alfred, NY 14802, USA
2) School of Materials Science and Engineering, Xi'an University of Architecture and Technology, Xi'an 710055, China
3) Institute of General and Inorganic Chemistry, Uzbekistan Academy of Sciences, Tashkent 100170, Uzbekistan

(Received: 2 December 2009; revised: 20 January 2010; accepted: 9 February 2010)

Abstract: Magnesia (MgO) is widely used in the production of refractory materials due to its high melting point, high thermal shock, and excellent slag resistance. The properties of refractory materials depend upon magnesia sources and processing parameters. In this work, three different magnesium sources, namely, magnesium hydroxide concentrate, magnesium carbonate concentrate, and intermediate flotation concentrate, were obtained from the Zinelbulak talc-magnesite, Uzbekistan, by causticization-hydration and flotation processes, respectively. A series of refractory materials were prepared on the basis of these magnesium sources, and their effects on physico-mechanical properties and microstructures were investigated as a function of sintering temperature, molding pressure, and the particle size of magnesium sources. The experimental results showed that a refractory material obtained from the magnesium hydroxide concentrate at 1600°C for 4 h demonstrated favorable parameters due mainly to a higher degree of contact among fine particles. The results obtained from X-ray diffraction and optical microscopy confirmed the presence of periclase and forsterite as the predominant phases in refractory specimens. The prepared refractory materials meet the requirements of the State Standards (Nos.4689–94 and 14832–96) for magnesia and forsterite refractories, respectively. It is, therefore, suggested herein that the use of different magnesium sources derived from the Zinelbulak talc-magnesite will offer the potential to provide economic benefits in the refractory industry.

Keywords: refractory materials magnesia; mechanical properties; microstructure; sintering

1. Introduction

Magnesium oxide, also known as magnesia, is one of the most widely used refractory materials for lining furnaces, ladles, glass-tank checkers, and secondary refining vessels in ferrous and nonferrous metallurgy, due to its high degree of refractoriness, the ability to withstand thermal shock, and excellent slag resistance [1-3]. Along with these, it has also been applied in various fields as an excellent heat- and electric-resistant and robust material, as well as a good conductor of heat. Until now, tremendous amounts of research work have been done on the enhancement of physico-mechanical, thermal, and chemical properties, lowering sintering temperature, and the reduction in the production cost of magnesia-containing refractories, including periclase-chromite [4], periclase-lime [5], periclase-nitride [6], and periclase-alumina [7].

According to the research of Borisenko *et al.* [8], presently, the manufacturers of magnesia-containing refractories are cutting down the production of periclase-chromite, periclase-lime, dinas, semi-acid, and chamotte refractories, and in turn, increasing the rate of production in periclase-carbide refractories owing to their quality of high refractoriness and the ability to resist erosion and corrosion of metals and oxides; however, their resistance capacity and service reliability strongly depend on the quality of the carbonaceous binder. On the contrary, Banerjee *et al.* [9] has recently described that the carbon content of the refractories is not environment-friendly and additional expenses may arise to conduct a stringent process of quality control when antioxidants, coatings, and binders are excessively used. They suggested a prospective route for preparing unshaped re-

---

Corresponding author: Mirabbos Hojamberdiev E-mail: mirabbos_uz@yahoo.com

fractories with the assistance of a nanocrystalline spinel through a modified sol-gel method. Othman and Khalil [10] demonstrated the use of less expensive raw materials with highly expensive spinel and MgO-C refractories in order to produce sintered or chemically bonded magnesia-containing bricks possessing a high degree of efficiency and excellent refractoriness.

However, at present, due to the mounting concern over economy, for the resumption of the refractory industry in Uzbekistan, it becomes imperative and crucial to search for new magnesia-containing raw materials located within the country. When the Zinelbulak talc-magnesite deposit was first discovered in the early 1920s, it was merely investigated as a filler for the production of insecticides [11]. It was much later that Tabachkova *et al.* [12] manufactured a sawed refractory material possessing a density of 2.92 g/cm^3, a compressive strength of 8.3-21.6 MPa, and the refractoriness of 1550-1750°C directly from the talc-magnesite without any purification. It is known that the impurities present in raw materials can ultimately affect the quality of refractory products, the extent of their application area, and their lifespan. Hence, it was important to concentrate talc and magnesite concentrates from the Zinelbulak talc-magnesite to manufacture refractory products with enhanced quality. In our previous work [13], the talc and magnesite concentrates were separated from Zinelbulak talc-magnesite by applying gravity concentration, flotation, and magnetic separation. However, the impurities with relatively low fraction were still present even after the flotation process, which eventually hinders their use in the production of periclase refractory. Therefore, the objective of the present study is to investigate the Zinelbulak talc-magnesite in detail, to obtain different magnesium sources, and to study their effects on the physico-mechanical properties of refractory materials as a function of sintering temperature, molding pressure, and particle size of magnesium sources.

2. Experimental

2.1. Starting materials

The talc-magnesite samples were collected from the Zinelbulak deposit, western Uzbekistan. The samples were first crushed by a jaw crusher, milled by a ball mill, and then subjected to a conventional flotation process, as described in detail elsewhere [13]. An experimental procedure is represented in Fig. 1. The conversion rate of magnesium oxide into magnesium hydroxide was determined by estimating weight loss against temperature from thermogravimetric (TG) curves. In order to investigate the sinterability of caustic magnesia obtained from magnesium hydroxide concentrate (MHC) and magnesium carbonate concentrate (MCC), apparent porosity and linear shrinkage were determined based on the ASTM Standard Method [14-15]. To study the effect of the particle size of magnesium sources on the sinterability of refractory samples, the sieved powders were classified into the following groups: <0.05, 0.05-0.09, 0.09-0.5, and 0.5-1 mm.

2.2. Preparation of refractory samples

A series of refractory specimens were prepared on the basis of the classified powders of MHC, MCC, and intermediate flotation concentrate (IFC) in the form of a briquette (25 mm×25 mm×125 mm) with 3wt% alkyd resin (as a binder), dried at 110°C for 24 h, and sintered at 1500 and 1600°C for 4 h. The effects of sintering temperature (1500-1600°C), molding pressure (80-100 MPa), and particle size on the physico-mechanical properties of refractory specimens were investigated. Linear shrinkage, bulk density, apparent porosity, water adsorption, compressive strength, and the degree of refractoriness expressed under load were determined according to the standard methods [14-17]. The Archimedes method was applied using kerosene as the immersion fluid.

2.3. Characterization

The chemical compositions of the samples (wt%) were determined by the wet chemical method. The densities of the powdered samples were measured by an AccuPyc 1330 helium pycnometer (Micromeritics, USA). The crystalline phases were detected using a D/MAX2550V X-ray diffractometer (Rigaku, Japan) with monochromated Cu K_α radiation. The differential thermal analysis (DTA)/thermogravimetric analysis (TGA) was performed on a Derivatograph Q-1500 (MOM, Hungary) within 20-1000°C at a heating rate of 10°C/min under a static atmosphere. The micrographs of the specimens with varied magnifications (×100, ×300, ×320, and ×1000) were taken with MIN-8 (LOMO, Russia) and Nikon E600 POL (Nikon, Japan) optical microscopes equipped with a digital camera.

3. Results and discussion

3.1. Petrographic analysis of talc-magnesite

An intensive examination of the varied forms of iron oxides present in the Zinelbulak talc-magnesite is imperative to find an effective way to reduce the content of iron oxides in the magnesite concentrate. For this purpose, the

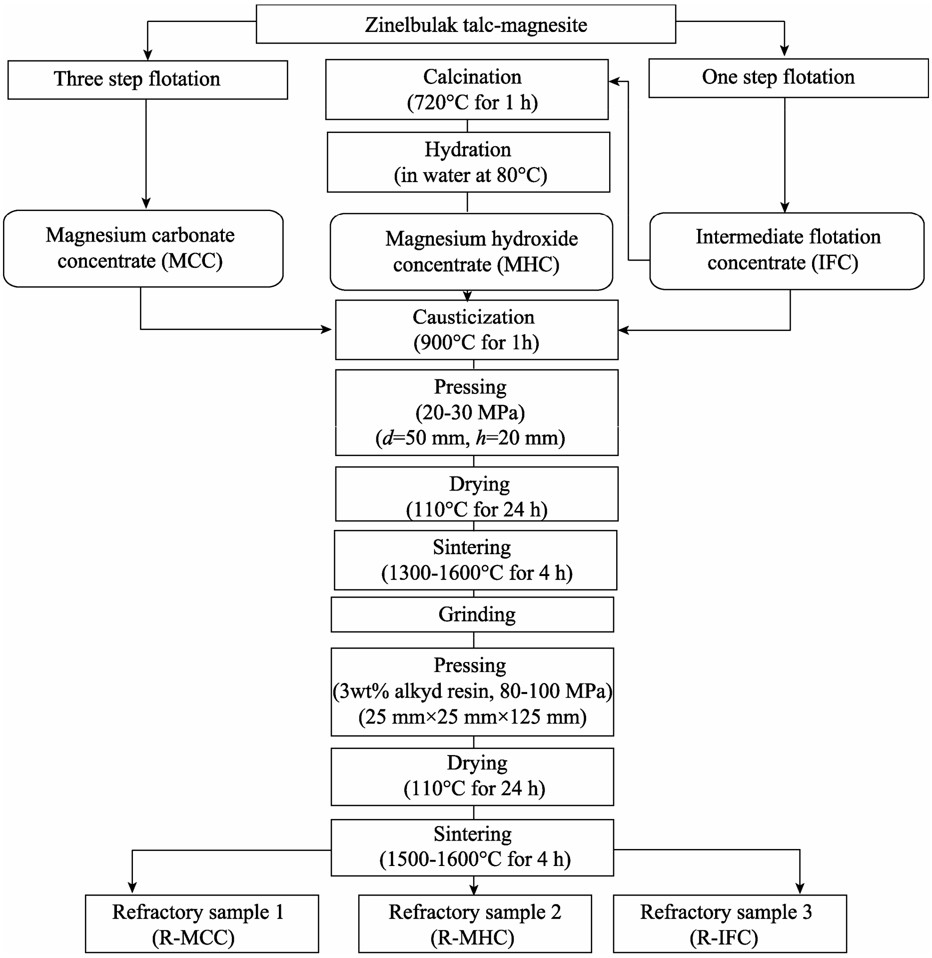

Fig. 1. Schematic representation of the processing of refractory materials.

talc-magnesite samples were first subjected to petrographic analysis. The petrographic images of the samples are illustrated in Fig. 2. The presence of a twisted boundary line between the particles of magnesite (the blue area) and talc (the cyan and purple areas) can be distinctly observed in Fig. 2(a). It shows that black magnetite particles are distributed in the form of a placer with an irregular shape; as in magnesite, it is also highly nonuniform, and it reflects a wide range in the distribution of particle size in talc. Evidently, the color of the magnesite area changes from blue (as seen in Fig. 2(a)) to violet or brown (Fig. 2(b)) due to the isomorphous substitution of magnesium ions (Mg^{2+}) by the divalent ions of iron (Fe^{2+}) within the crystal structure of magnesite. Further, this substitution led to the formation of breunnerite $[(Mg,Fe^{2+})CO_3]$ in the Zinelbulak talc-magnesite. The brown particles of magnesite are found to be irregularly distributed just as a spill and a limbus on the boundaries of the magnesite and talc particles. The intensity of this brown color substantiates the almost high degree of isomorphous substitution of Mg^{2+} by Fe^{2+}, that is, 5% to 30%, within the crystal lattice of magnesite. The results of the petrographic analysis of the talc-magnesite reveal the major issue associated with obtaining a high-quality magnesite concentrate by the processes of flotation and magnetic separation owing to a dense coalescence of the fine crystals of talc and magnesite and a large proportion of very fine particles of magnetite. As reported previously [13], the intermediate flotoconcentrate contains 34wt%-37wt% MgO, 21wt%-25wt% SiO_2, 1wt%-2wt% CaO, and 6wt%-8wt% Fe_2O_3. However, the content of impurities can be considerably decreased only after the third step of flotation.

3.2. Causticization-hydration process of the intermediate flotation concentrate

As it is evident in Fig. 3, the first small endothermic peak formed at 490°C in the DTA curve of the intermediate flotoconcentrate concentrate is assigned to the dehydration process of siderite ($FeCO_3$), the second endothermic effect appeared at 680°C corresponds to the decarbonization process of magnesite ($MgCO_3$), and the third endothermic peak

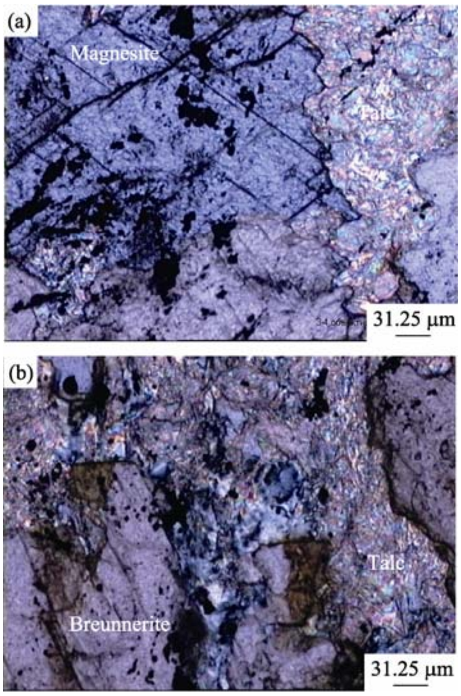

Fig. 2. Petrographic images of the Zinelbulak talc-magnesite: (a) magnesite-talc-rich region; (b) breunnerite-talc-rich region.

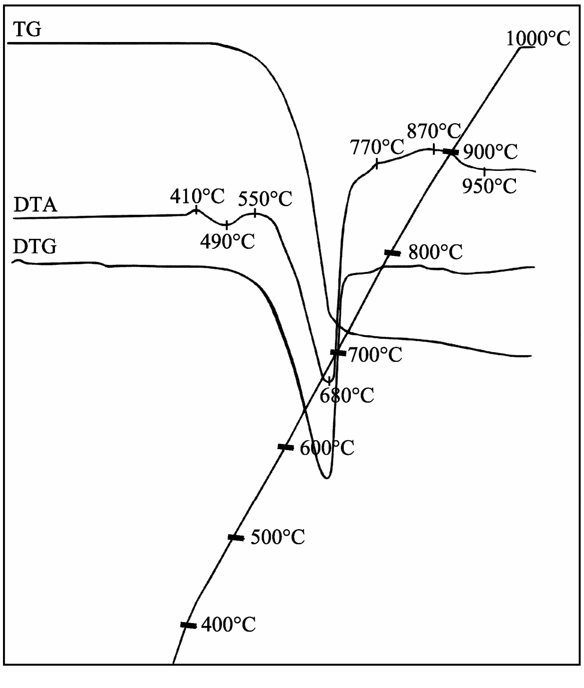

Fig. 3. DTA-TG curves of the intermediate flotation concentrate obtained from the Zinelbulak talc-magnesite.

centered at 950°C is attributed to the dehydration process of talc [$Mg_3Si_4O_{10}(OH)_2$]. When the intermediate flotation concentrate was further heated up, the structural water was drained-off, the last traces of water were lost, and the talc broke down into enstatite ($2MgO{\cdot}2SiO_2$) and cristobalite (SiO_2), as expressed by

$$2Mg_3Si_4O_{10}(OH)_2 \rightarrow 3Mg_2Si_2O_6 + 2SiO_2 + 2H_2O.$$

The total weight loss of the Zinelbulak talc-magnesite is >22%. Generally, the intensive loss of water in talc occurs at 900-1100°C. At a temperature of around 770°C, the newly created magnesium oxide reacts with silicate minerals and consequently forms a low-temperature form of magnesium metasilicate (clinoenstatite) containing chains of connected SiO_4 tetrahedra:

$$2SiO_2 + 2MgO \rightarrow Mg_2Si_2O_6.$$

Therefore, 720°C was chosen as an optimum causticizing temperature of the intermediate flotation concentrate. As mentioned above, a higher degree than this optimum temperature can however decrease the potency of MgO to undergo a hydration process due to the phases that resulted from the reaction of magnesium oxide and silicates. The magnesium hydroxide content, the amount of bound water, and the conversion degree of magnesium oxide into magnesium hydroxide estimated from the TG curves are plotted in Fig. 4 as a function of time. Evidently, the hydration process of caustic magnesia concludes (100%) after 72 h. With an increase in the content of the bound water to 14.85wt%, the content of magnesium hydroxide gradually reaches 48.4wt%. The high amount of magnesium hydroxide formed during the hydration process is closely related to the enhanced degree of solubility of MgO at 80°C. On one hand, the degree of solubility of MgO is quite high at a high temperature. On the other hand, the degree of solubility of magnesium hydroxide lessens with an increase in temperature. According to Rocha *et al.* [18], the reaction mechanism for this process mainly comprises the adsorption of water on the surface, the processes of intraparticle diffusion, oxide dissolution within the particles, the creation of super-saturation, nucleation, and the growth of magnesium hydroxide crystallites at the oxide surface, as given by the following reaction:

$$MgO(s) + H_2O(l) \rightarrow Mg(OH)_2(s).$$

The hydration rate is controlled by the dissolution rate of MgO and the diffusion of OH^- ions, which strongly depends on the pH value. In the experiment conducted in the present study, the hydration process of MgO occurs at a pH value of 10±0.5 and can be significantly decreased in a strong basic pH region due to a low degree of solubility of MgO [19]. It should also be mentioned here that an extremely rapid

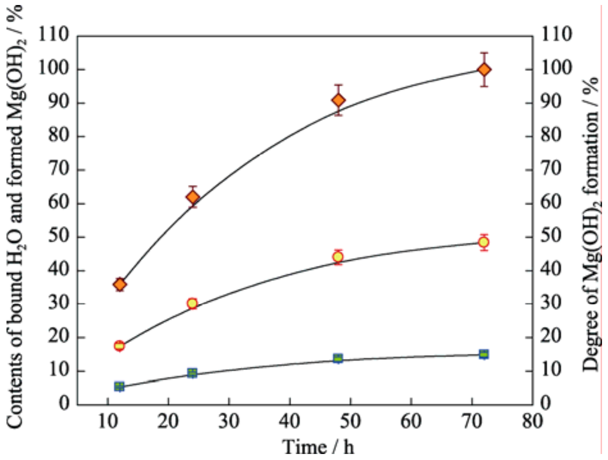

Fig. 4. Contents of bound H_2O (rectangle) and formed $Mg(OH)_2$ (circle), and the degree of $Mg(OH)_2$ formation (diamond) as a function of time.

hydration rate of magnesia will result in the formation of relatively larger magnesium hydroxide aggregates, which comprise submicroscopic crystallites of a wider surface area—a particle morphology that is not acceptable for some applications [20].

3.3. Sinterability of caustic magnesia

The chemical compositions of the Zinelbulak talc-magnesite, intermediate flotation concentrate, magnesium carbonate concentrate, and magnesium hydroxide concentrate are listed in Table 1. The content of magnesium oxide varies according to the applied processing methods, and it eventually reaches the maximum value (66.24wt%) only after being subjected to the cauterization-hydration process. In this case, the content of the existing impurities is appreciably decreased (SiO_2: 1.78wt%; Fe_2O_3+FeO: 2.13wt%).

Table 1. Chemical compositions of various magnesium sources derived from the Zinelbulak talc-magnesite wt%

Product	SiO_2	Al_2O_3	Fe_2O_3+FeO	CaO	MgO	K_2O	Na_2O	L.O.I.
Natural talc-magnesite	34.0	0.94	6.84	0.70	34.6	0.03	0.04	22.85
Magnesium hydroxide concentrate (MHC)	1.78	0.58	2.13	0.59	66.24	0.10	0.36	28.22
Magnesium carbonate concentrate (MCC)	2.42	0.90	7.49	0.38	41.96	0.15	0.61	46.09
Intermediate flotation concentrate (IFC)	22.7	0.84	6.33	0.98	35.68	0.20	1.04	32.23

Note: L.O.I.— loss on ignition.

The sinterability of the pellet-shaped caustic magnesia obtained from two different magnesium sources (MHC and MCC) was investigated as a function of temperature, ranging from 1300 to 1600°C for 4 h. As shown in Fig. 5, the sintering parameters of the MHC samples are found to be significantly higher in comparison with those of the MCC samples. The difference that appears in the values of the parameters of the two samples remarkably increases with an increase in sintering temperature. The mean size of periclase grains is larger in the MHC samples than that in the MCC samples at 1600°C. The maximum values of apparent porosity and linear shrinkage of the MHC and MCC samples are 12.4% and 23.1% (Fig. 5(a)) and 14.8% and 17.6% (Fig. 5(b)), respectively, at the final sintering temperature of 1600°C. A decrease in apparent porosity and an increase in linear shrinkage at a high temperature might be attributed to the volume- and grain-boundary diffusion and the elimination of the surface. At the beginning, the rate of linear shrinkage is fast; however, it slows down with an increase in temperature. This means that when the neck radius found between the particles is minute and the contact area between them is entirely limited, so the rate of linear shrinkage is comparatively rapid. However, as the expanse of the contact area increases and the neck radius becomes larger, the rate of linear shrinkage decreases quite drastically [21]. It is well known that along the grain boundaries, the disorder among particles is more rapid than the diffusion through the crystalline lattice, *i.e.*, the atoms on the surface of a solid are more mobile than those on the lattice sites within the crystal volume. The average size of periclase grains is 1.5 times greater than that of the initial periclase crystals in the caustic magnesia obtained from the MHC sample. In contrast, the average size of periclase grains in the sample obtained from the MCC sample is much smaller. Because silicates form a viscous fluid in the reaction with iron oxide, and instead of assisting the process, it usually hinders the growth of periclase crystals. Nevertheless, the iron oxide acts as a flux forming a ferromagnesian compound that melts and increases the conversion rate of the remaining magnesia into periclase, which is most stable at higher temperatures. The sintering and recrystallization abilities of periclase are higher in the MHC samples due to the larger specific surface area of the precipitated superfine magnesium hydroxide and a higher degree of contact of the sintering particles.

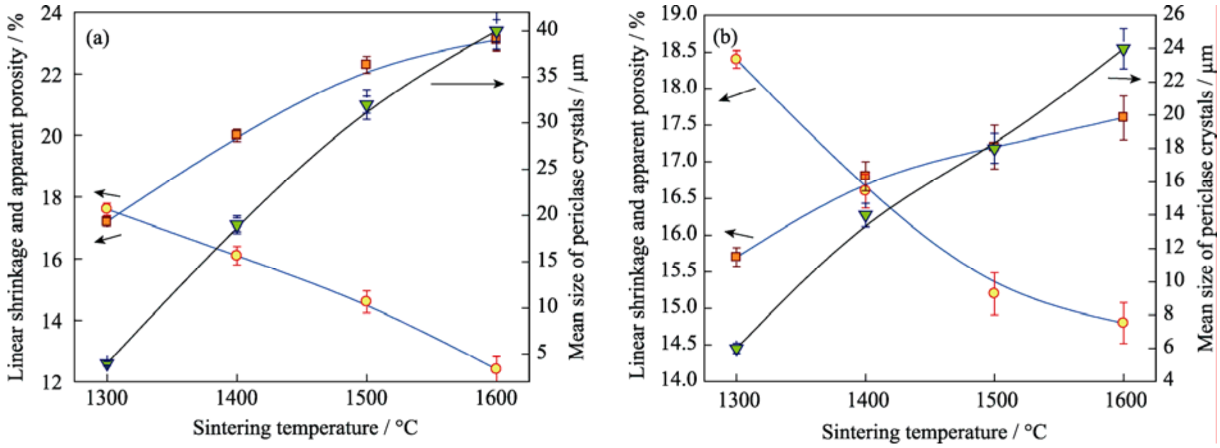

Fig. 5. Linear shrinkage (rectangle), apparent porosity (circle), and the mean size of periclase crystals (triangle) of the samples based on caustic magnesia derived from magnesium hydroxide concentrate (a) and magnesium carbonate concentrate (b) as a function of temperature.

Table 2 shows the chemical compositions and densities of the powders obtained after the pellets being sintered at 1500°C for 4 h. Based on its chemical composition, the magnesia powder obtained from the MHC sample meets the requirement criteria of the State Standard (No.10360–85) established for identifying the highest category. Correspondingly, the powder derived from the MCC sample meets the requirement criteria of the first category set by the State Standard; however, it has a relatively low content of MgO and comparatively high amounts of SiO_2 and Fe_2O_3. The chemical composition of the powder obtained from the IFC sample proves that it is favorable for the production of the forsterite refractory.

3.4. Physico-mechanical properties of refractory samples

The physico-mechanical properties of the refractory samples, namely, linear shrinkage, compressive strength, water absorption, bulk density, apparent porosity, and the degree of refractoriness expressed under load, are given in Table 3. It is evident from the table that the physico-mechanical properties of the refractory specimens derived from magnesium hydroxide (R-MHC) and magnesium carbonate (R-MCC) were quite similar in comparison with the sample derived from the intermediate flotation concentrate (R-IFC). It shows that the values of linear shrinkage, compressive strength, degree of refractoriness under load, and bulk density increase, whereas those of water adsorption and apparent porosity decrease with an increase in sintering temperature and molding pressure. In particular, all these properties reflect higher values for the R-MHC and R-MCC samples, along with the addition of a larger proportion of fine particles (<0.05 mm). A pronounced change is evidently noticed in the physico-mechanical properties of the samples when the sintering temperature is raised up to 1600°C. In addition, the values of bulk density for the R-MCC samples are higher than those for the R-MHC samples. The main reason for this difference might be the high content of iron oxide, conesquently forming a larger number of heavy minerals at high temperatures. Further, higher values of linear shrinkage and bulk density, along with lower values of apparent porosity and water adsorption are recorded for the R-MCC samples at 1600°C. This evidently substantiates the formation of a large amount of the silicate glassy matrix in the R-MCC samples due to the higher content of the oxides of silicon, aluminum, sodium, and iron that act as fluxes and accelerators during the reaction [22]. However, the silicate glassy matrix ultimately decreases a softening temperature (or refractoriness) and creeping of the refractory products during exploitation. The lowest value of water absorption and a

Table 2. Chemical composition and densitiy of the hard-burnt powders derived from different magnesium sources at 1500°C for 4 h

Sample	Chemical composition/wt%							Density/ $(g\cdot cm^{-3})$
	SiO_2	Al_2O_3	CaO	MgO	Fe_2O_3+FeO	K_2O	Na_2O	
MHC	2.43	1.07	0.74	92.17	2.97	0.24	0.38	2.90
MCC	4.66	1.62	0.82	80.35	11.61	0.25	0.69	3.21
IFC	32.69	1.26	1.25	54.06	8.97	0.29	1.48	3.18

Table 3. Physico-mechanical properties of the refractory specimens obtained from different magnesium sources

Sample	Tempera-ture/°C	Pressure applied / MPa	Particle size distribution / %				Linear shrinkage / %	Compressive strength / MPa	Water adsorption / %	Bulk density / (g·cm^{-3})	Apparent porosity / %	Refractoriness (under the load of 9.8 N) / °C
			1.0-0.5 mm	0.5-0.09 mm	0.09-0.05 mm	<0.05 mm						
Refractory from magnesium hydroxide concentrate (R-MHC)	1500	80	20	20	20	40	2.71	46.2	14.9	2.74	18.1	1560
			20	30	20	30	2.63	44.9	15.3	2.69	17.2	1550
		100	20	20	20	40	2.77	48.1	14.3	2.89	16.8	1570
			20	30	20	30	2.70	47.7	14.8	2.78	17.0	1560
	1600	80	20	20	20	40	2.92	50.2	13.0	3.10	15.1	1585
			20	30	20	30	2.84	49.0	14.2	3.08	16.7	1570
		100	20	20	20	40	2.95	52.8	12.1	3.36	13.9	1590
			20	30	20	30	2.91	50.1	13.9	3.29	16.2	1580
Refractory from magnesium carbonate concentrate (R-MCC)	1500	80	20	20	20	40	2.90	47.3	15.1	3.26	17.0	1550
			20	30	20	30	2.75	46.9	16.2	3.19	18.0	1540
		100	20	20	20	40	2.82	49.9	13.9	3.39	16.4	1555
			20	30	20	30	2.78	48.9	15.3	3.28	17.4	1550
	1600	80	20	20	20	40	3.02	48.6	14.2	3.34	16.7	1560
			20	30	20	30	3.34	46.8	15.8	3.26	17.8	1555
		100	20	20	20	40	3.11	50.7	13.9	3.41	16.2	1565
			20	30	20	30	3.15	49.6	14.7	3.36	16.7	1560
Refractory from intermediate flotation concentrate (R-IFC)	1500	80	20	20	20	40	3.34	29.8	13.8	3.26	16.1	1545
			20	30	20	30	3.45	28.6	14.1	3.20	16.5	1540
		100	20	20	20	40	3.47	32.7	13.1	3.29	15.3	1550
			20	30	20	30	3.55	30.9	13.3	3.26	16.0	1545
	1600	80	20	20	20	40	3.59	35.7	12.7	3.29	14.8	1555
			20	30	20	30	3.54	32.6	12.9	3.21	14.9	1550
		100	20	20	20	40	3.51	36.4	12.4	3.37	14.2	1560
			20	30	20	30	3.54	33.2	12.7	3.28	14.7	1555

relatively high value of apparent porosity for the R-MHC samples are attributed to the densification of the specimen through a collective recrystallization of the small periclase crystallites in periclase grains. Probably, a small content of the silicate glassy matrix induces a relatively higher value of apparent porosity in spite of the increase in sintering temperature. Meanwhile, linear shrinkage and bulk density of the R-MHC sample remain relatively low due to the small content of the glassy matrix and the formation of magnesium ferrite ($MgFe_2O_4$), respectively. The role played by the formed silicate glassy matrix, in particular, is evident in the R-IFC samples. Further, the R-MCC and R-IFC samples reveal the high values of linear shrinkage and bulk density, which abruptly increase with an increase in the temperature to 1600°C, regardless of the parameters of molding pressure and the particle size of the powders. Water absorption and apparent porosity decrease to their lowest values for all three samples at the final temperature. A lower rate of compressive strength and refractoriness of the specimens is directly related to the formation of a lesser amount of periclase and magnesium ferrite crystals during the formation of forsterite (Mg_2SiO_4) and the silicate glassy matrix, respectively. The crystals of forsterite completely enclose the periclase crystals, binding them firmly together, and hence, forming a very strong mass (Figs. 6(d)-(e)). It also shows that the bonds formed in the magnesia

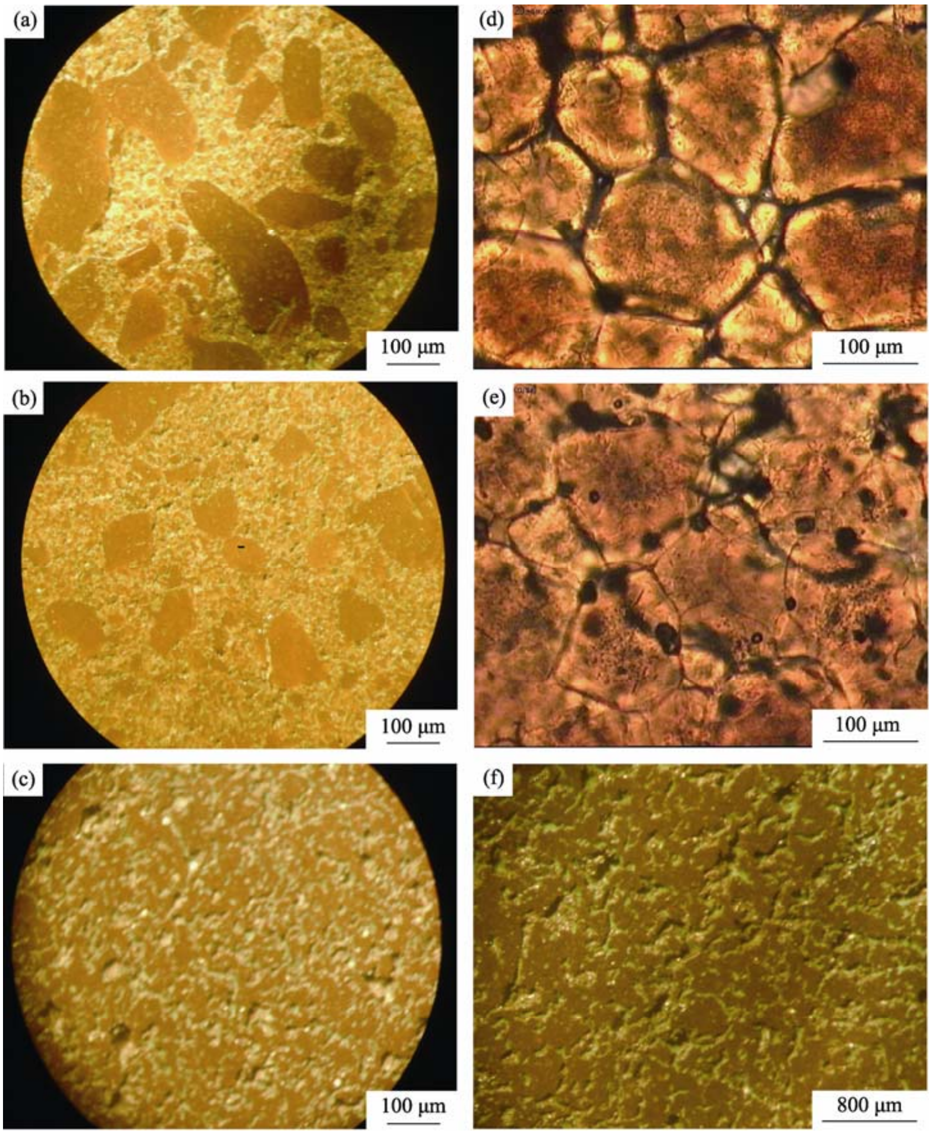

Fig. 6. Optical micrographs of the refractory specimens prepared at 1600°C for 4 h from magnesium hydroxide concentrate (a) (d), magnesium carbonate concentrate (b) (e), and intermediate flotation concentrate (c) (f).

refractories are mainly resulted from a glassy matrix containing a large part of impurities, which surrounds the rounded crystals of periclase (Figs. 6(d) and (e)). This bond is found to consist almost completely of forsterite. Ordinarily, silica is combined with magnesia to form forsterite and iron with magnesia to form spinel in the refractory samples, as given by the following equations:

$2MgO+SiO_2 \rightarrow Mg_2SiO_4$;

$MgO+Fe_2O_3 \rightarrow MgFe_2O_4$.

In this experiment, a consistent change in the physico-mechanical properties of the samples is observed depending on the magnesium sources used, the particle size of the powders, molding pressure, and sintering temperature. Among the three samples, the R-MHC samples based on 20% of 1.0-0.5 mm, 20% of 0.5-0.09 mm, 20% of 0.09-0.05 mm, and 40% of <0.05 mm powders, which were pressed under 100 MPa and sintered at 1600°C for 4 h, exhibits the best parameters.

The increased value of apparent porosity is considered to be caused by a low degree of contact between the particles of the powders of lower specific surface area (in the MCC sample). In comparison with the R-MHC and R-MCC samples, the R-IFC sample has a higher bulk density and lower apparent porosity and compressive strength. In fact, the production of a high amount of iron-containing minerals causes an increase in density and the rate of formation of the silicate glassy matrix, which is contributed by a sufficient amount of the ions of sodium, calcium, and aluminum as cation-modifiers with a high content of SiO_2. The R-MHC sample reflects favorable properties that conform to the requirements of the State Standard (No.4689–94) established for the periclase refractory.

3.5. Microstructure of the refractory samples

As seen in Fig. 6(a), the R-MHC samples are characterized by the presence of small crystals of periclase (<50 μm), along with a large number of periclase grains in the background. Such a collective recrystallization of small crystals in the periclase grains reveals their excellent sinterability at a sufficient temperature and holding time. The R-MCC samples are also found to be distinguished by the presence of small crystals scattered in the periclase grains; however, these grains have a relatively smaller size (Fig. 6(b)) in comparison with those in the R-MHC sample. Some of the separated pores are also found in these samples to exist in an irregular shape with the size of 100-500 μm and in a wave-like shape with the size of 200-250 μm. In Fig. 6(c), the structure of the R-IFC sample is specified by the uniformly patterned image in which the twisted lines of conglomerates of the forsterite and magnesium ferrite crystals are present. They are dark brown and surrounded by the light brown glassy matrix of the silicates of magnesium and iron. Moreover, the pond-like pores in the size of 0.1-0.3 mm can also be seen in Fig. 6(f).

Figs. 6(d)-(e) represent the micrographs of the R-MHC and R-MCC samples, respectively. A marked difference can be observed in the content of black spots, where magnesium ferrite is found to be highly concentrated. The glassy matrix is formed by the silicates in order to build up thin borders around the large crystals of periclase. The pores are found to be present in a relatively small size in these samples. Further, the presence of a high content of magnetite in magnesium carbonate leads to formation of an increased amount of magnesium ferrite in the R-MCC sample. The microstructure of the R-MCC sample differs significantly in the degree of magnification (Fig. 6(e)), *i.e.*, the rounded-angular shaped periclase crystals are somewhat fewer. Hence, they are adjacent to each other with the formation of a monolithic structure. Black dot-like inclusions are present in the magnesium ferrite crystals and connect each other through the winding lines. The XRD analysis (not shown here) reveals that the periclase is a predominant phase in the R-MHC and R-MCC samples, and the intensity of magnesium ferrite peaks is quite weak in the R-MHC sample in comparison with that of the R-MCC sample. The microstructures of the refractory specimens examined by petrographic analysis demonstrate the formation of the well-crystallized periclase in the R-MHC sample. The prepared refractories containing periclase and forsterite conform to the requirements of the State Standards (Nos.4689–94 and 14832–96) established for the magnesia and the forsterite refractories, respectively.

4. Conclusions

(1) The petrographic analysis of the talc-magnesite confirmed the presence of breunnerite [$(Mg,Fe^{2+})CO_3$], which formed as a result of the isomorphous substitution of magnesium ions (Mg^{2+}) by divalent iron ions (Fe^{2+}) in the crystal structure of magnesite.

(2) The conversion of magnesium oxide derived from the intermediate flotation concentrate by calcination at 720°C for 1 h into magnesium hydroxide was completed after 72 h when kept in distilled water at 80°C. The caustic magnesia obtained from the magnesium hydroxide concentrate at

1500°C for 4 h showed high sinterability.

(3) The refractory specimens (R-MHC) based on the magnesium hydroxide concentrate demonstrated optimum physico-mechanical properties owing to the high degree of contact among fine particles, along with a higher specific surface area.

(4) The results obtained from X-ray diffraction and optical microscopy revealed that periclase and forsterite were the main crystal phases in the prepared refractory specimens (R-MHC, R-MCC, and R-IFC), respectively.

(5) The prepared refractory specimens met the requirements of the State Standards (Nos.4689–94 and 14832–96) for magnesia and forsterite refractories, respectively. The use of various magnesium sources derived from the Zinelbulak talk-magnesite offers economic benefits in the refractory industry.

Acknowledgement

MH thanks the Fulbright Program for the award of a research fellowship under which the present study was partially carried out.

References

[1] R. Amavis, *Refractories for the Steel Industries*, Elsevier Applied Science, New York and London, 1990.

[2] P.P. Budnikov, *The Technology of Ceramics and Refractories*, M.I.T. Press, Cambridge, 2003.

[3] S. Banerjee, *Monolithic Refractories: A Comprehensive Handbook*, Wiley-American Ceramic Society, Westerville, 1998.

[4] V. Petkov, P.T. Jones, E. Boydens, B. Blanpain, and P. Wollants, Chemical corrosion mechanisms of magnesia-chromite and chrome-free refractory bricks by copper metal and anode slag, *J. Eur. Ceram. Soc.*, 27(2007), p.2433.

[5] Y.A. Dmitrienko, R.S. Polovinkina, and N.G. Koval, Advanced periclase-lime powders for converter refractories, *Refract. Ind. Ceram.*, 40(1999), p.120.

[6] Y.W. Li, S.L. Jin, Y.B. Li, L. Zhao, and Z.Y. Li, Microstructural evolution in MgOp/AlN composites, *Ceram. Int.*, 35(2009), p.2241.

[7] G.I. Antonov, A.V. Kushchenko, O.M. Semenenko, and G.N. Shcherbenko, Synthesis of magnesia-alumina spinel using periclase and bauxite, *Refract. Ind. Ceram.*, 32(1991), p.499.

[8] O.N. Borisenko, G.D. Semchenko, M.A. Chirkina, and I.V. Kasymova, High-strength periclase-carbon refractories based on phenol-formaldehyde resin with modification of different batch components, *Refract. Ind. Ceram.*, 47(2006), p.225.

[9] A. Banerjee, S. Das, S. Misra, and S. Mukhopadhyay, Structural analysis on spinel ($MgAl_2O_4$) for application in spinel-bonded castables, *Ceram. Int.*, 35(2009), p.381.

[10] A.G.M. Othman and N.M. Khalil, Sintering of magnesia refractories through the formation of periclase-forsterite-spinel phases, *Ceram. Int.*, 31(2005), p.1117.

[11] T.N. Dalimov, T.S. Shayakubov, and V.I. Troitskiy, *Geology and Minerals of Uzbekistan*, University Press, Tashkent, 1998.

[12] S.N. Tabatchikova, I.A. Stepanova, T.N. Kudryavtseva, F.I. Ismailov, and S.L. Mudryi, Talc-magnesite rocks from the Zinel'-Bulaksk deposits as raw material for the production of refractories, *Refractories*, 25(1984), p.639.

[13] M. Hojamberdiev, P. Arifov, K. Tadjiev, and Y. Xu, Characterization and processing of talc-magnesite from the Zinelbulak deposit, *Min. Sci. Technol.*, 20(2010), p.415.

[14] ASTM C20-00, Standard test method for apparent porosity, water absorption, apparent specific gravity, and bulk density of burned refractory brick and shapes by boiling water, [in] *Annual book of ASTM Standards*, Vol.15.02, West Conshohocken, PA, 2006.

[15] ASTM C356-03, Standard test method for linear shrinkage of preformed high-temperature thermal insulation subjected to soaking heat, [in] *Annual book of ASTM Standards*, Vol. 04. 06, West Conshohocken, PA, 2000.

[16] ASTM C773-88, Standard test method for compressive (crushing) strength of fired whiteware materials, [in] *Annual book of ASTM Standards*, Vol.15.02, West Conshohocken, PA, 2005.

[17] GOST 4069-69, *Method of Refractoriness Determination*, State Committee of Standards, Moscow, 1970.

[18] S.D.F. Rocha, M.B. Mansur, and V.S.T. Ciminella, Kinetics and mechanistic analysis of caustic magnesia hydration, *J. Chem. Technol. Biotechnol.*, 79(2004), p.816.

[19] O. Fruhwirth, G.W. Herzog, I. Hollerer, and A. Rachetti, Dissolution and hydration kinetics of MgO, *Surf. Technol.*, 24(1985), p.301.

[20] D. Filippou, N. Katiforis, N. Papassiopi, and K. Adam, On the kinetics of magnesia hydration in magnesium acetate solutions, *J. Chem. Technol. Biotechnol*, 74(1999), p.322.

[21] V.K. Singh and U.K. Mandal, Densification of mixes of calcium dialuminate and monoaluminate, *J. Mater. Sci. Lett.*, 4(1985), p.627.

[22] I.B. Cutler, Sintered alumina and magnesia, [in] A.M. Alper ed. *Refractory Materials*, Academic Press, New York and London, 1970, p.129.